Resolution of a Multi-Step Electron Transfer Reaction by Time Resolved Impedance Measurements: Sulfur Reduction in Nonaqueous Media

Jin-Bum Park, Byoung-Yong Chang, Jung-Suk Yoo, Sung-Young Hong, and Su-Moon Park*

*Department of Chemistry and Center for Integrated Molecular Systems, Pohang University of Science and Technology, Pohang, Gyeongbuk 790-784, Korea. *E-mail: smpark@postech.edu*

The first reduction peak of the cyclic voltammogram (CV) for sulfur reduction in dimethyl sulfoxide has been studied using time resolved Fourier transform electrochemical impedance spectroscopic (FTEIS) analysis of small potential step chronoamperometric currents. The FTEIS analysis results reveal that the impedance signals obtained during short potential steps can be resolved into electron transfer reactions of two different time constants in a high frequency region. The FTEIS method provides snap shots of impedance profiles during an earlier phase of the reaction, leading to time resolved EIS measurements. Our results obtained by the FTEIS analysis are consistent with a series of electron transfer and chemical equilibrium steps of a complex reaction, making up an ECE (electrochemical-chemical-electrochemical) mechanism postulated from the results of computer simulation.

Key Words : Electrochemical impedance spectroscopy (EIS), Fourier transform EIS (FTEIS), ECE, Equivalent circuit

Introduction

Many multiple-step electron transfer reactions appear to occur in a single step as can be seen from their single voltammetric peaks, and it is often impossible to resolve them into each electron transfer step although it is well understood that multiple-electron transfer reactions would not occur in a single step in a concerted manner.[1,2] An example includes the metal electrodeposition from its ions such as in
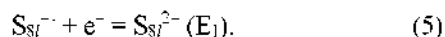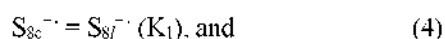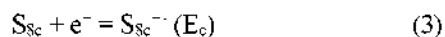
$$Zn^{2+} + 2e^- \rightarrow Zn, \tag{1}$$
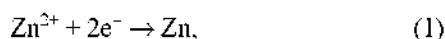
in which a two-electron transfer reaction appears to occur in a single step in its voltammogram and/or polarogram. This type of reaction has not been resolved into each electron transfer step by a known electrochemical technique even though it has been well understood that a single step concerted two-electron transfer would not be possible.[1,2] The kinetic analysis does not help much because only the rate determining step of the two steps would be represented in the kinetic expression of such a reaction in a traditional electrochemistry experiments.

A cyclic octamer of sulfur, S_{8c}, has been reported to undergo a two electron transfer reaction to produce its dianion according to[3-6]

$$S_{8c} + 2e^- = S_{8c}^{2-}. \tag{2}$$

which is followed by a series of following chemical and electrochemical reactions to produce a number of products.[7-9] Levillain *et al.*[10,11] proposed an electrochemical-chemical-electrochemical (ECE) mechanism for this one-step two-electron reduction from their computer simulation study of the first peak of its cyclic voltammogram, in which the first reduction peak was postulated to be made of a series

of ECE reactions as follows:

$$S_{8c} + e^- = S_{8c}^{-} \ (E_c) \tag{3}$$

$$S_{8c}^{-} = S_{8l}^{-} \ (K_1), \text{ and} \tag{4}$$

$$S_{8l}^{-} + e^- = S_{8l}^{2-} \ (E_1). \tag{5}$$

Here $E_1^0 > E_c^0$ (more positive) and also S_{8c}^{-} generated in the very first step according to reaction (3) not only undergoes an equilibrium reaction to S_{8l}^{-} (reaction (4)) but transfers its electron to S_{8l}^{-} to produce S_{8l}^{2-}, which is not shown in the above reaction series. Here subscripted "*l*" denotes a linear chain sulfur molecule. While it is quite reasonable that the reaction would be made of more than one step considering that a concerted two-electron transfer reaction is not probable as already described above,[1,2] there has been no experimental evidence for the proposed mechanism other than the result of computer simulation.[10,11] This is because the second reaction (reaction (5)) occurs at a potential more positive at a faster rate than the first reaction.

In the present work, we demonstrate that a multi-electron transfer reaction can be resolved into each step employing time resolved impedance measurements obtained by FTEIS analysis of transient currents. In order to demonstrate that the resolution is possible, sulfur reduction in a nonaqueous medium was chosen as its electron transfer rate is relatively sluggish.

Experimental

All the samples were prepared and handled in an argon-filled glove box to avoid contamination by moisture and oxygen. Sulfur (powder, Aldrich, 99.98%), tetrabutylammonium perchlorate (TBAP, Fluka, ≥99%), and dimethyl sulfoxide (DMSO; anhydrous, Aldrich, 99.9%) were used

for preparation of solutions without further purifications.

A single-compartment cell housing a platinum disk working electrode with its diameter of 1.8 mm (geometric area = 0.025 cm^2), a platinum foil counter electrode, and a home-made Ag/AgNO$_3$ (in 0.010 M AgNO$_3$ in DMSO) reference electrode was used for the electrochemical measurements. The working electrode was polished to a mirror finish successively with alumina slurries (Buehler) of 5.0 down to 0.05 μm. After the solution was prepared in a glove box. the experiments have been run outside the box in an argon atmosphere by continuously purging the cell above the solution with argon through a small hole through a tightly fitted Teflon cell cap.

The impedance measurements were made by applying a sequence of descending potential steps of 15 mV every 150 ms in a potential range of −0.60 to −1.20 V with a home-built potentiostat having a slew rate of 20 MV/s. The current was sampled at a rate of 500.000 samples/s after the application of each potential step. Staircase voltammograms were constructed from the thus obtained data by sampling currents at a given sampling time, 2 ms.

After the data acquisition, both the potential and the chronoamperometric current packets were segmented according to each step function. Impedances were computed from currents recorded for 150 ms by taking the first derivatives of the step voltage and the resulting currents. followed by fast Fourier transform (FFT) of the derivative signals with frequencies ranging from $1/t_{total}$ to $1/(2\Delta t)/30$. The Nyquist theorem states that the frequency should range between $1/t_{total}$ and $1/(2\Delta t)$, but the upper frequency limit was set at $1/(2\Delta t)/30$ because the currents at frequencies higher than $1/(2\Delta t)/30$ were found to contain significant noise. Here Δt is the sampling interval and $t_{total} = N \cdot \Delta t$, where N is the total number of samples. The FFT calculations were carried out using a Matlab program (MathWorks, Natick, MA), and circuit simulations were conducted to fit the observed values to the proposed equivalent circuits using an EG&G's ZSimpWin program. This program uses a CNLS procedure to obtain the global minimum of the χ^2 function with a modulus weighting. All the frequencies corresponding to 2^n times of the lowest frequency ($1/t_{total}$ or 6.67 Hz). were included in the plot. where n is an increasing integer starting from 0. until the upper limit. $1/(2\Delta t)/30$. was reached.

The impedance was also measured by using a Solartron model 1255 frequency response analyzer (FRA) at a given bias potential applied by an EG&G model 273 potentiostat-galvanostat. both of which were controlled by a Pentium PC through IEEE-488 bus. An ac signal of 10 mV (peak-to-peak) was overlaid on the bias potential and the ac current data were acquired at a rate of 10 points per decade during the frequency scan between 10 kHz and 6 Hz.

Results and Discussion

Impedance measurements have been used to resolve a series of electron transfer reactions due to their capability of observing reactions of different kinetics in different fre-

quency domains.[12] The impedance of the electrode-electrolyte interface is represented by an equivalent circuit, in which a charge transfer resistance (R_{ct}) and a double layer capacitance (C_{dl}) are connected in parallel in its simplest form. at the time of charge transfer across the double layer capacitor, and its RC time constant represents the kinetics of the reaction. Thus far, only slow reactions such as corrosion reactions have been resolved by showing that the impedance data can be represented by more than one RC circuit of different time constants. This is because the reactions took longer than the time taken for impedance measurements when the reactions are slow enough. Generally, it took a long time to measure an impedance spectrum in a full frequency range by traditional impedance measurement techniques. in which ac waves of various frequencies are scanned in the same way as in traditional spectroscopic measurements. In recent years, however, techniques of time resolved impedance measurements began to be developed using a concept of Fourier transform electrochemical impedance spectroscopy (FTEIS).[13-22] FTEIS experiments can be run in two different modes. A more straightforward approach is to mix ac waves of known frequencies and apply the mixed signal packet to an electrochemical system.[13-21] The current signal obtained thereof is then resolved back into the ac current of each frequency by Fourier transform and used for impedance calculation. This method, first developed by Smith et al. in the seventies,[13-19] has been optimized recently thanks to recent advances in electronics and used during cyclic voltammetric scans by overlaying a signal packet on a sweep signal.[20,21] Another technique takes advantage of the fact that a Dirac δ function is made of ac waves of *all* frequencies with an identical initial phase and amplitude.[22] Thus, the current obtained upon application of the δ function to an electrochemical system would contain ac currents of *all* frequencies. leading to the calculation of impedances in a full frequency range. However, no electronic device is presently available for the generation and application of an ideal δ function, which led to the use of its integrated form, *i.e.*, small potential step instead. The first derivative of the small potential step used as an excitation signal and a chronoamperometric current obtained thereof are then converted to the ac voltage and current data using Fourier transform. and the impedance data are obtained by dividing the ac voltage by the ac current at desired frequencies.[22a,b,d] Advantages of this technique include among others that impedance data are obtained from transient currents. leading to the snap shots of impedance profiles at the time of electron transfer at a potential before the step has been applied.[22c,e]

Cyclic Voltammetric and Chronocoulometric Experiments. Figure 1a shows a typical cyclic voltammogram (CV) recorded for reduction of 3.0 mM sulfur at a platinum disk electrode in a DMSO solution containing 0.10 M TBAP. The electrochemical behavior of sulfur reduction has been studied extensively. and the CV shown here is in excellent agreement with those reported in the literature.[3-11] The absence of cathodic shoulders between the first and
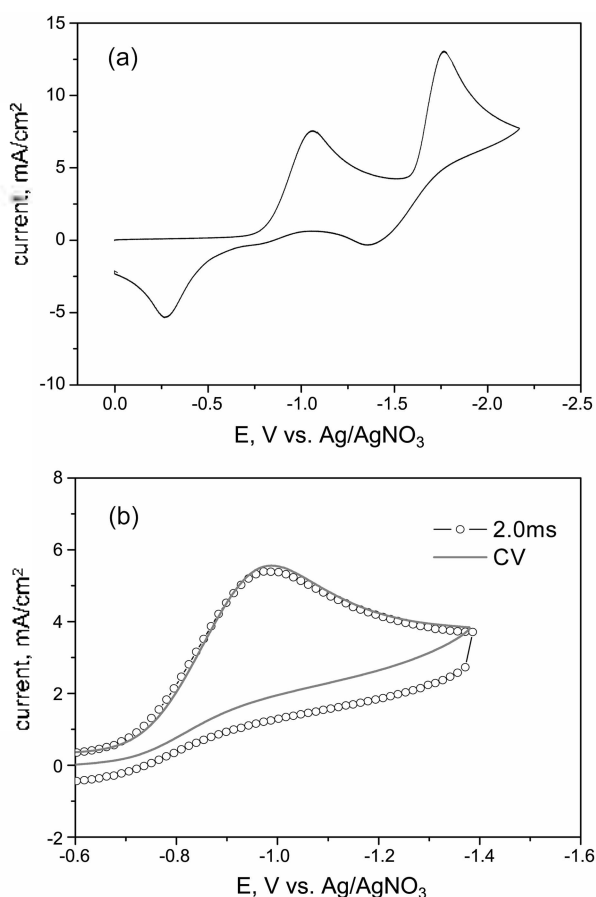
Figure 1. (a) Cyclic voltammogram recorded at a scan rate of 100 mV/s for reduction of 3.0 mM sulfur in DMSO containing 0.10 M TBAP, and (b) staircase voltammograms constructed from currents sampled at a sampling times of 2 ms (−○−), and a CV (dashed line) for the first reduction step of sulfur. The step height was 15.0 mV with a step period of 150.0 ms.

Figure 2. Chronocoulometric response curve for reduction of 3.0 mM sulfur. The initial potential was stepped from 0 to −1.10 V vs. Ag/AgNO₃ for 100 ms.

second reduction peaks, whose peak potentials are −1.04 and −1.77 V vs. Ag/AgNO₃, evidences that the DMSO used in our present work is clean and free of water.[8] An expanded CV recorded for the first reduction peak at 100 mV/s (dotted line) between −0.6 and −1.35 V and the corresponding staircase cyclic voltammogram (SCV) (−○−) assembled by plotting the currents sampled at 2.0 ms from the series of chronoamperometric currents are shown in Figure 1b. Both the SCV and CVs indicate that sulfur reduction is electrochemically and chemically irreversible as the peak potential shifts in a negative direction at shorter sampling times or faster scan rates (not shown) and almost no anodic peak is observed upon potential scan reversal. Thus, no immediate reduction product is reoxidized upon reversing the potential within the potential range scanned. The anodic peak at about −0.25 V shown in Figure 1(a) is due to oxidation of secondary product(s) produced from the immediate reduction product obtained at the first and/or second reduction peaks.[7,8] The anodic peak does not decay to 0 as the secondary products keep diffusing in toward the electrode surface for oxidation even above 0.0 V.

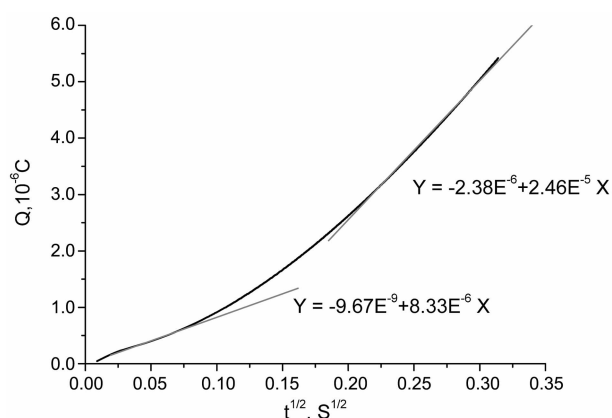In order to see whether the sulfur adsorption would

present any problems in the interpretation of impedance results for sulfur reduction, we ran a chronocoulometric experiment. The total charge recorded during a chronocoulometric experiment in a diffusion limited potential region, $Q_d(t)$, has an expression,[23]

$$Q_d(t) = \frac{2nFADo^{1/2}D_s^*}{\pi^{1/2}} \cdot t^{1/2} + Q_{dl} - nFA\Gamma_s, \quad (6)$$

where n is the number of electrons transferred, F the Faraday constant, A the electrode area, D_o the diffusion coefficient of sulfur in our case, t the electrolysis time, Q_{dl} the capacitive charge due to the double layer charging, and Γ_s the faradaic charge for reduction of surface excess sulfur. Thus, a positive intercept should result from both the adsorption of an oxidant (S_{8c} in this case) and double layer charging on the charge (Q) axis in the Q vs. $t^{1/2}$ plot. Figure 2 shows a chronocoulometric response for sulfur reduction at −1.10 V for 100 ms. The plot is made of two linear regions, one between 0 and ~10 ms and the other beyond ~40 ms. The negative slope observed before ~10 ms should be due to overcoming an overpotential for the reaction, the rate of which becomes faster leading to a larger slope beyond about 40 ms. The small negative intercept of −9.7 × 10⁻⁹ C on the charge (Q) axis indicates that charges due to both double layer charging and sulfur adsorption are negligibly small. The relatively large negative intercept of −2.4 × 10⁻⁶ C beyond ~40 ms also suggests that the reaction is still slow and needs to overcome an activation barrier to get it going. Thus, the results show that the adsorption is not significant if present at all, does not complicate the reaction, and does not present an extra semicircle due to the adsorption in the equivalent circuit in the analysis of the impedance data below. We also ran the chronoamperometric experiment without sulfur; no charge was recorded during the experiment for a sizable length of time.

Impedance Measurements and Their Interpretations. Figure 3 shows a few Nyquist plots for electrochemical impedance spectra, which were obtained by the FTEIS method by treating the chronoamperometric currents sampled
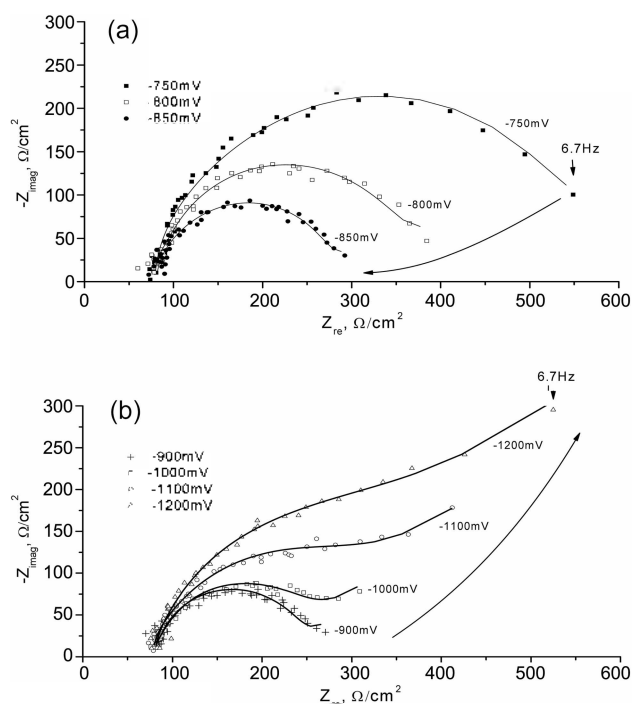
1526 *Bull. Korean Chem. Soc.* **2007**, Vol. 28, No. 9

Jin-Bum Park et al.

Figure 3. A few selected Nyquist impedance plots obtained by the FTEIS analysis of small step chronoamperometric currents in a potential range of: (a) −750 ~ −850 mV and (b) −900 ~ −1200 mV. The frequency range used for these data was between 6.7 Hz and 8.3 kHz.

Figure 4. A few selected Nyquist impedance plots obtained by the FRA method at: (a) −650 ~ −800 mV and (b) −850 ~ −1200 mV. The frequency range used for these data was between 6.0 Hz and 6 kHz.

for every 150 ms upon application of a series of 40 descending potential steps from −600 mV down to −1200 mV with a step height of 15 mV. Note that all 40 impedance spectra in a full frequency range of 8.3 kHz down to 6.7 Hz between −600 and −1200 mV were obtained in 6 s. It is observed in Figure 3 that the overall polarization resistance (R_p) decreases with the potential until it reaches −900 mV (Figure 3a) and then the Warburg impedance becomes increasingly important in determining the overall impedance plots beyond −1.0 V (Figure 3b). Here, we define R_p as $d\eta/di$ at a given overpotential η and distinguish it from R_{ct}, which is an R_p value at an equilibrium potential or $\eta = 0$.[22c,d] In the literature and even in most textbooks, these two are not clearly distinguished. The R_p values are obtained from the diameters of the semicircles in Nyquist plots. Here, semicircles in the Nyquist plots look somewhat depressed, indicating that more than one semicircles having different RC time constants must have been convoluted to give the observed impedance signals.[14-16] While surface roughness and/or porosity may also lead to slightly depressed semicircles, we have demonstrated that mass transport effects (Warburg impedance) cause semicircles to be slightly depressed at electrodes polished to as flat as 0.05 μm (50 nm).[22d] Since the Warburg impedance has been factored in our circuit simulation, the depressed semicircles must have resulted from more than one processes.

Figure 4 shows the impedance data obtained by the FRA method under otherwise exactly the same experimental conditions as used for FTEIS experiments: the semicircles
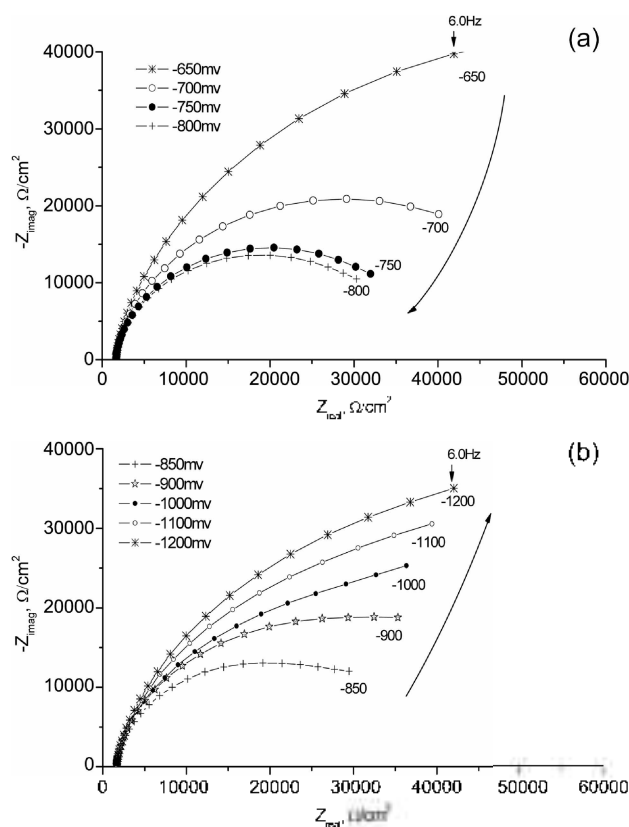
appear more severely depressed than those shown in Figure 3. It took more than 3 min to obtain a single spectrum at a given bias potential in the same frequency range as that used for the data shown in Figure 3, i.e., 10 kHz to 6 Hz, in a well optimized experiment, which took 150 ms in FTEIS experiments. In general, the Nyquist plots are more depressed and dominated by Warburg impedances, and polarization resistances are significantly larger when obtained at the same potential. These observations indicate that the electrochemical system must have undergone a series of following chemical reactions after the first electron transfer and all these electron transfer reactions have been integrated into the signals during the FRA measurements, resulting in heavily convoluted signals. It was for this reason that many questions have been raised in the literature as to the validity of the impedance data, when they were obtained by conventional methods, due to continuous changes taking place during the measurements, particularly when electron transfer reactions are irreversible.[20b,24-30]

Figure 5 shows three equivalent circuits (a-c) that have been used to fit the impedance spectra obtained over the whole potential range. The data shown in Figure 3 are best described by the first two circuits shown in Figure 5a and b, whereas those shown in Figure 4 can be fitted by the one shown in Figure 5c. The best fits were determined by trying to simulate impedance responses for a given circuit, which
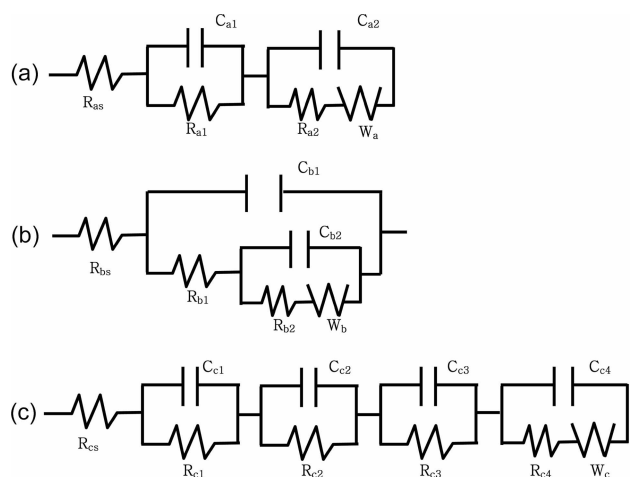
Figure 5. Proposed equivalent circuits for fitting the impedance data shown in Figures 3 and 4. Here R_{ji} is the solution resistance with subscripted i is a through c; R_{ij}, where subscripted i indicates a through c and j indicates I through 4, is the polarization resistance; C_{ij} are the double-layer capacitances; and W_i are the Warburg impedances.

gives the smallest χ^2-values between the fitted points and experimental data. The χ^2-value indicates the quantitative measure of the dispersion between the experimental data and the impedance responses generated from a given equivalent circuit. The smaller the χ^2-values are, the better the fit is between the simulated and observed data. Both circuits shown in Figures 5a and b gave identical χ^2-values for the whole potential region for the data shown in Figure 3. We thus conclude that what appeared to be a single-step electron transfer in the first reduction CV peak is actually made of two semicircles of different RC time constants.

Of the two equivalent circuits shown in Figure 5a and b, the one shown in b with two capacitors connected in parallel seems more reasonable for the reasons discussed below. The rate of the second electron transfer *must* be faster than that of the first because its standard electrode potential would be more positive than or equal to that of the first for an EE or ECE reaction when two CV peaks were perfectly merged into one.[10,11] Otherwise, two separate reduction peaks would have been observed in a CV or SCV rather than a single peak.[1] This is one of criteria for the examination of the impedance analysis results employing two circuits shown in Figure 5a and b. Another criterion is that the R_p value should decrease upon increase in overpotential as the Butler-Volmer (B-V) equation indicates. The B-V equation has an expression in its simplified form.[1,2,22c]

$$i - i^0 \left(e^{\frac{\alpha n F \eta}{RT}} - e^{\frac{(1-\alpha)n F \eta}{RT}} \right) \tag{7}$$

Here i^0 is an exchange current, α is a cathodic transfer coefficient, η is an overpotential defined as $E-E_{eq}$ with E_{eq} being an equilibrium potential, and other symbols have their usual meanings. The relation between R_p and η is readily seen when the definition of R_p ($=d\eta/di$) is realized as already described above.
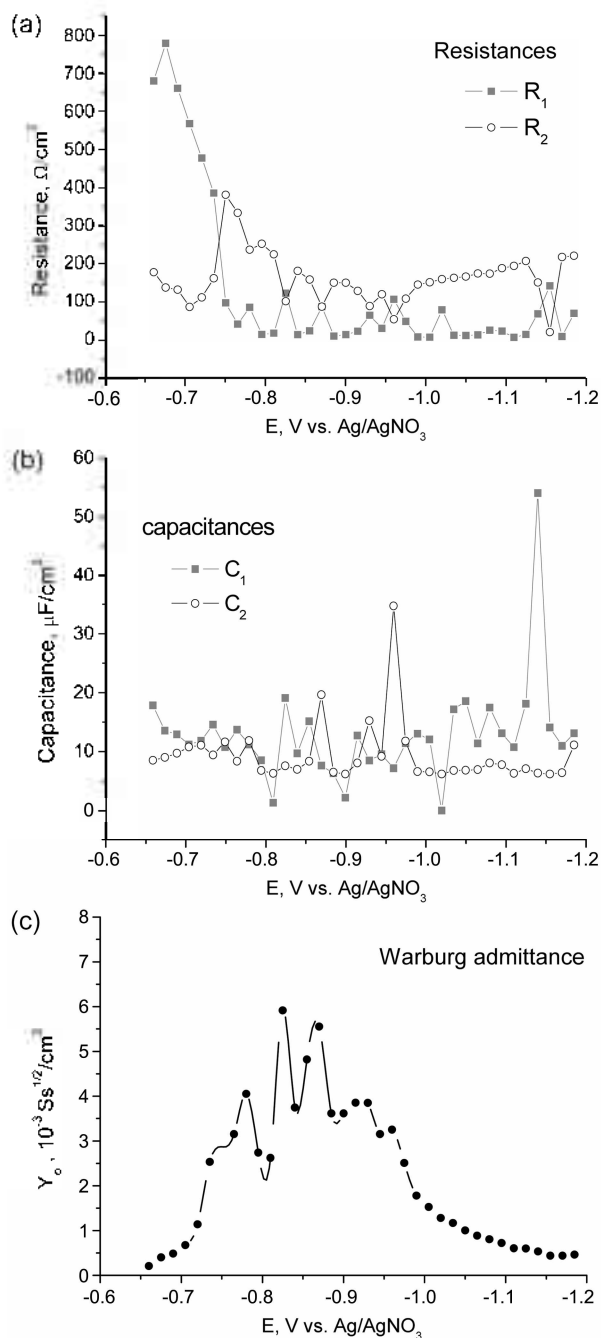

Figure 6. Results of impedance analysis obtained at potentials from −650 to −1200 mV using the equivalent circuit shown in Figure 5a for the data obtained by the FTEIS analysis: (a) polarization resistances (R_p), (b) capacitances (C), and (c) Warburg impedances (W) plotted against potential.

The results of impedance analysis obtained from the two equivalent circuits in Figure 5a and b are shown in Figures 6 and 7. First, the behaviors of polarization resistances (R_1 and R_2) obtained from the first equivalent circuit shown in Figure 5a, which are shown in Figure 6a, are not consistent with those expected from a normal B-V behavior: both R_1 and R_2 should decrease exponentially as the overpotential increases as discussed above. Here, R_2 does not change as expected from a typical electrochemical reaction activated by an
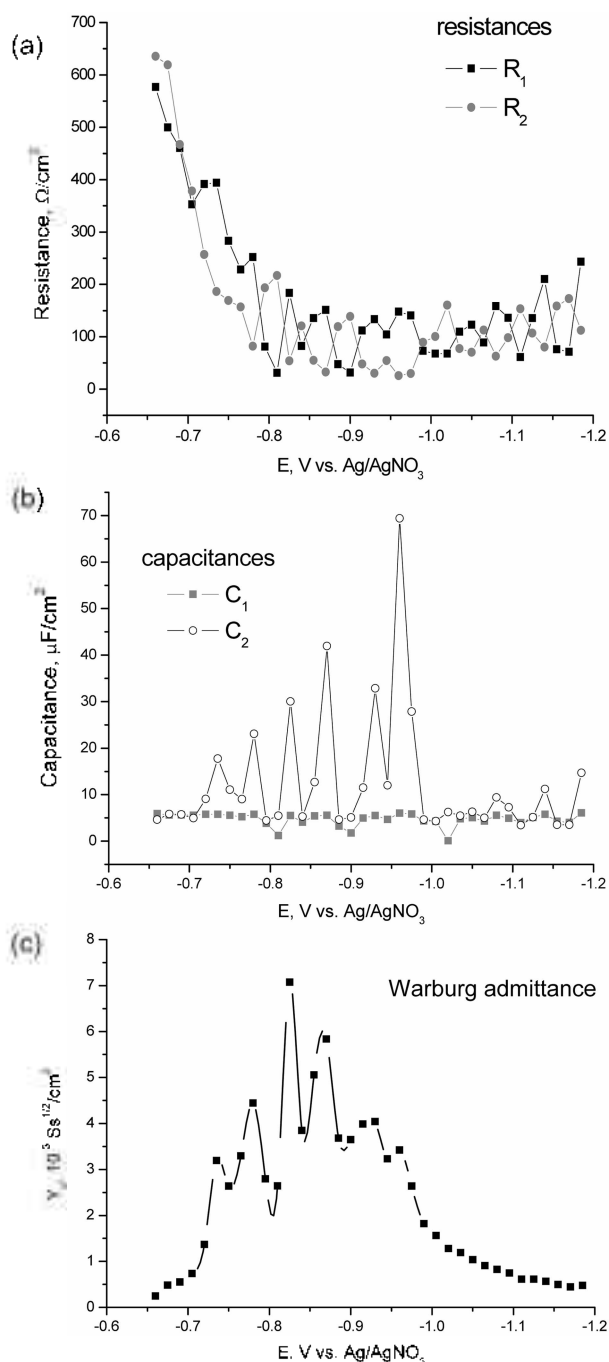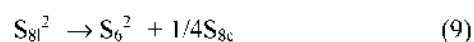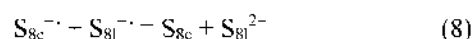
Figure 7. Results of impedance analysis obtained at potentials from −650 to −1200 mV using the equivalent circuit shown in Figure 5b for the same data as used for Figure 6: (a) polarization resistances (R_p), (b) capacitances (C), and (c) Warburg impedances (W) plotted against potential.

increase in overpotential. However, the results shown in Figure 7a, which were obtained from the second equivalent circuit in Figure 5b, are consistent with the overpotential-activated mechanism for two reasons. First, both resistances, R_1 and R_2, decay exponentially for an increase in over-potential. Second, R_2 is in general slightly smaller than R_1, indicating that the second electron transfer reaction must be more facile than the first although it fluctuates at higher overpotentials.

Another observation is that C_2 shown in Figure 6b fluctuates rather randomly in the data obtained from the serial capacitance circuit (Figure 5a), whereas rather periodical fluctuations are observed in Figure 7b before the potential reaches −1.0 V; however, C_1 stays nearly constant over the wide range of potential for both cases. The pattern shown by the data in Figure 7b is more consistent with the physical picture as discussed below. The charged ions produced in the double layer accumulate until their total concentration reaches a critical value to initiate a series of following electron transfer and/or chemical reactions as summarized below[3-11]:

$$S_{8c}^{-\cdot} - S_{8l}^{-\cdot} - S_{8c} + S_{8l}^{2-} \tag{8}$$

$$S_{8l}^{2-} \rightarrow S_6^{2-} + 1/4 S_{8c} \tag{9}$$

$$S_6^{2-} - 2 S_3^{-\cdot}, \text{ and} \tag{10}$$

$$S_{8l}^{2-} \rightarrow 2S_3^{-\cdot} + 1/4 S_{8c}. \tag{11}$$

Once the chemical reactions are initiated as summarized by reactions (8)-(11), the amount of charged species would decrease leading to a decrease in capacitance as the products are less charged than the reactants. This would repeat on the electrode surface, and rather periodic increases and decreases in capacitances would be observed as shown in Figure 7b.

Another evidence for these repeated reactions is shown by the oscillatory behavior shown by the Warburg impedances. Due to the production of readily reducible neutral substances and their subsequent reduction according to the series of reactions summarized by (8) through (11), the impedance due to the mass transport would also fluctuate in a similar way to the variation of the double layer capacitance. The oscillatory behaviors shown by the Warburg admittances obtained from the impedance data are displayed in Figures 6c and 7c. This sequence would repeat periodically on the electrode surface providing the oscillatory behaviors as shown in Figure 6b as well as Figures 6c and 7c. The Warburg admittances are obtained from an equation,[31]

$$Y_{\text{if}} - \frac{\sqrt{\omega}}{\sqrt{2} \cdot \sigma} \tag{12}$$

where ω is $2\pi f$ with f being frequency and σ is defined as

$$\sigma = \frac{RT}{\sqrt{2} n^2 F^2 A} \left(\frac{1}{\sqrt{D_O} \cdot C_O(0,t)} + \frac{1}{\sqrt{D_R} \cdot C_R(0,t)} \right) \tag{13}$$

Here D is a diffusion coefficient of the subscripted species (oxidant or reductant), $C(0,t)$ is the concentration of the subscripted species at the electrode surface, and other symbols have their usual meanings. The parameter σ is obtained from the dependence of real or imaginary impedance on frequency. The Warburg admittance shows a peak value at a potential corresponding to E^0 (formal potential),[32] and a few peaks are seen in both Figures 6c and 7c, indicating that more than one electron transfer reactions are taking place. At higher overpotentials beyond about −1.0 V, the rate of reduction is so large that all the species near the electrode surface would be reduced indiscriminately, resulting in much smaller fluctuations as shown in Figures 6c, 7b, and 7c.
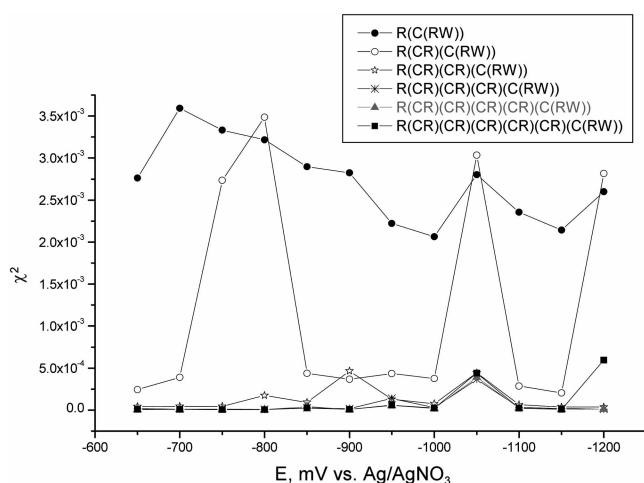
Figure 8. χ^2 vs. E plot for the data shown in Figure 4 using equivalent circuits shown in Figure 5c.

FTEIS measurements were also made at different scan rates to check if the oscillations in Warburg admittances indeed resulted from the potential dependency or a simple time dependency. When we ran the experiments at higher scan rates of 50 mV/s and 100 mV/s, the frequency of the oscillations went down correspondingly (results not shown here), indicating that the phenomena show a more time than potential dependent nature.

Finally, Figure 8 shows the χ^2-values plotted as a function of the bias potential for fitting a series of equivalent circuits to the impedance data obtained by the FRA method shown in Figure 4. The result indicates that the χ^2-values converge to their minima with a circuit containing at least four semicircles, suggesting that as many as four or more electron transfer reactions must be taking place during the measurements. The best fitting equivalent circuit is chosen such that a circuit would have the smallest χ^2-values at all potentials with the smallest number of RC units.

Two important differences between the data taken by FTEIS and FRA methods are the time taken for the data acquisition for the same frequency range and the way the overpotential is applied. For the FTEIS method, the data acquisition time is 150 ms at a given bias potential corresponding to the lowest frequency of 6.7 Hz, while it takes more than 180 s by the FRA method with the lowest frequency set to 6.0 Hz, which is about 1200 times of the former. The relatively long time taken here is primarily due to the relatively lengthy waiting period until a steady state current is reached upon application of a larger magnitude potential step and the time taken for averaging signals at each frequency. Thus, the data acquisition time becomes longer for an electrochemically unstable system whose current signal fluctuates or decreases continuously as the machine waits until the current settles down.

Another important difference is that a small excitation wave made of all ac waves (*i.e.*, a *small* and *fast* potential step) is applied at a bias potential of −900 mV, for example, in the FTEIS experiments where the concentration profiles have been established for a certain period, whereas a *large*

magnitude potential step of −900 mV is applied with ac waves of various frequencies used subsequently as excitation sources. Thus, the changes in impedances during the series of reactions, whose time constants fall within the longest sampling period, are all integrated over the time the data acquisition is taken. For this reason, only two reactions, whose time constants are shorter than 150 ms, are observed during the FTEIS measurements while all the reactions that occur within more than about 180 s period would be observed during the FRA measurements. Thus, a two-electron transfer reaction is observed during the FTEIS measurements, while reactions of four or five different time constants are observed as can be seen from Figure 8.

Another distinctive difference is the domination of the Warburg component in the data obtained by the FRA method as seen from Figures 3 and 4 because a single large step is applied and the system goes into the mass transport limited mode immediately. As has been reported,[7-9] many following reactions occur after the first electron transfer at the first reduction peak as summarized above and subsequent electron transfer reactions thereof are all observed as a convoluted signal. Reaction products generated in the first reduction peak include S_8^{2-}, S_6^{2-}, S_4^{2-}, S_3^{2-}, and S_7· as well as fragmented small sulfur molecules due to further reduction of products obtained from reactions (6)-(9).[7-9] Of these, both S_3· and S_7·, as well as neutral sulfur molecules of various sizes, can accept further electrons in this potential range, giving rise to the oscillatory behaviors shown in Figures 6c, 7b, and 7c.

In an electrochemical system undergoing a series of following chemical reactions and subsequent electron transfer reactions to or from the products formed thereof, the number of reactions having different RC time constants in the equivalent circuit used for fitting the impedance data would be a function of the sampling period used for the experiment. To show that this is the case, we extended the sampling period of our FTEIS measurements to 1000 ms (= 1 Hz) and the result indicated that three semicircles were needed for fitting the impedance data (data not shown). In other words, the data obtained in a reasonably short sampling period of 150 ms were shown to require two semicircles of two different RC time constants, while three electron transfer reactions were needed for fitting the data when the sampling period was extended to 1 s. On the other hand, the data obtained in a longer sampling period, >180 s in the FRA method, required at least four semicircles as shown in Figure 8.

Unfortunately, we were not able to determine the exchange rate constants for the two subsequent electron transfer reactions from our impedance data because standard electrode potentials are not known for the two electron transfer reactions, and we are not able to compare the exchange rate constants of the two electron transfer steps with those obtained from the computer simulation.[10,11] When the standard electrode potentials are available, the exchange rate constants and other electrokinetic data can be obtained rather straightforwardly from the impedance data by plotting the

polarization resistance (R_p) as a function of overpotential, and the R_p-value at the overpotential of 0, or at the standard electrode potential, allows the exchange current or rate constant to be calculated.[1,2,30,32] However, we were not able to obtain standard electrode potentials for two electron transfer reactions, (3) and (5), in our case because the free energies of formation of the immediate reduction products, are neither available nor can be determined.

Conclusion

In our present work, we have demonstrated for the first time that snap shots of impedances taken by FTEIS analysis of small step chronoamperometric currents during an electrochemical reaction offer an excellent way to experimentally resolve what appears to be a single step multi-electron transfer reaction. To our knowledge, this is the first attempt at resolving a multi-step electron transfer reaction employing real time EIS measurements although a general theory has been developed for impedance behaviors for such systems.[33,34] We chose the first electron transfer step of sulfur reduction, which has been postulated to undergo a two-step electron transfer reaction with a chemical equilibrium intervening in between, *i.e.*, *via* an ECE mechanism. The equivalent circuit describing the measured impedance data required two to as many as four or five RC time constants depending on the sampling period and the method of measurements. The two RC time constants observed by the FTEIS measurements is consistent with the proposed mechanism for the first reduction peak *via* an ECE mechanism.

We should emphasize in this work that an important contribution of this work is the attempt to resolve what appears to be a single step multi-electron transfer reaction using real time EIS measurements. We should also point out that the FTEIS technique in impedance measurements has analogy to the time resolved spectroscopy in spectroscopic measurements similar to a transient spectroscopic tool, although it still is in its primitive stage. While we have examined the reaction, in which an ECE mechanism is operative in our current work, we may be able to extend our approach to elementary steps of many other faster single step multi-electron transfer reactions with an EE mechanism when the technique is fully developed. In the technique, both the potentiostats and data acquisition systems must be fast enough to follow reactions in high frequency regions.

References

1. Bard, A. J.; Faulkner, L. R. *Electrochemical Method*, 2nd ed.;
Wiley & Sons: New York, 2001; Chapters 2, 3, 4, and 12.
2. Bockris, J. O. M.; Reddy, A. K. N.; Gamboa-Aldeco, M. *Modern Electrochemistry*, 2nd ed.; Kluer Academic/Plenum Publishers: New York, 2000.
3. Martin, R. P.; Daub, W. H. J.; Robert, J. L.; Sawyer, D. T. *Inorg. Chem.* **1973**, *12*, 1921.
4. Badoz-Lamling, J.; Bonnaterre, R.; Cauquis, G.; Delamar, M.; Demange, G. *Electrochim. Acta* **1976**, *21*, 119.
5. Baranski, A. S.; Fawcett, W. R.; Gilbert, C. M. *Anal. Chem.* **1985**, 57.
6. Evans, A.; Montenegro, M. I.; Pletcher, D. *Electrochem. Commun.* **2001**, *3*, 514.
7. Kim, B.-S.; Park, S.-M. *J. Electrochem. Soc.* **1993**, *140*, 115.
8. Han, D.-H.; Kim, B.-S.; Choi, S.-J.; Jung, Y.; Kwak, J.; Park, S.-M. *J. Electrochem. Soc.* **2004**, *151*, E283.
9. Bonnaterre, R.; Cauquis, G. *J. C. S. Chem. Comm.* **1972**, 293.
10. Levillain, E.; Gaillard, F.; Leghie, P.; Demortier, A.; Lelieur, P. *J. Electroanal. Chem.* **1997**, *420*, 167.
11. Leghie, P.; Lelieur, J.-P.; Levillain, E. *Electrochem. Commun.* **2002**, *4*, 406.
12. *Impedance Spectroscopy*, 2nd ed.; Barsoukov, E.; Macdonald, J. R., Eds.; Wiley Interscience: Hoboken, NJ, 2005.
13. Creason, S. C.; Smith, D. E. *J. Electroanal. Chem.* **1972**, *36*, 1.
14. Creason, S. C.; Smith, D. E. *Anal. Chem.* **1973**, *45*, 2401.
15. Smith, D. E. *Anal. Chem.* **1976**, *48*, 221A and 517A.
16. Schwall, R. J.; Bond, A. M.; Loyd, R. J.; Larsen, J. G.; Smith, D. E. *Anal. Chem.* **1977**, *49*, 1797.
17. Schwall, R. J.; Bond, A. M.; Smith, D. E. *Anal. Chem.* **1977**, *49*, 1805.
18. O'Halloran, R. J.; Schaar, J. E.; Smith, D. E. *Anal. Chem.* **1978**, *50*, 1073.
19. Czeszczuk, M.; Smith, D. E. *J. Electroanal. Chem.* **1983**, *157*, 205.
20. (a) Popkirov, G. S.; Schindler, R. N. *Rev. Sci. Instrum.* **1992**, *63*, 5366; (b) Popkirov, G. S.; Schindler, R. N. *Electrochim. Acta* **1993**, *38*, 861.
21. Darowicki, K.; Kawula, J. *Electrochim. Acta* **2004**, *49*, 4829.
22. (a) Yoo, J.-S.; Park, S.-M. *Anal. Chem.* **2000**, *72*, 2035. (b) Yoo, J.-S.; Song, I.; Lee, J.-H.; Park, S.-M. *Anal. Chem.* **2003**, *75*, 3294. (c) Park, S.-M.; Yoo, J.-S. *Anal. Chem.* **2003**, *75*, 455A. (d) Chang, B.-Y.; Park, S.-M. *Anal. Chem.* **2006**, *78*, 1052. (e) Park, S.-M.; Yoo, J.-S.; Chang, B.-Y.; Ahn, E.-S. *Pure Appl. Chem.* **2006**, *78*, 1069.
23. (a) Anson, F. C. *Anal. Chem.* **1966**, *38*, 54. (b) Christie, J. H.; Osteryoung, R. A.; Anson, F. C. *J. Electroanal. Chem.* **1967**, *13*, 236. (c) Chapter 5 of Ref. 1.
24. Sluyters-Rehbach, M.; Sluyters, J. H. *J. Electroanal. Chem.* **1979**, *102*, 415.
25. Stoynov, Z. B.; Savova-Stoynov, B. S. *J. Electroanal. Chem.* **1985**, *183*, 133.
26. Savova-Stoynov, B.; Stoynov, Z. B. *Electrochim. Acta* **1992**, *37*, 2353.
27. Stoynov, Z. *Electrochim. Acta* **1992**, *37*, 2357.
28. Stoynov, Z. *Electrochim. Acta* **1993**, *38*, 1919.
29. Urquidi-Macdonald, M.; Real, S.; Macdonald, D. D. *Electrochim. Acta* **1990**, *35*, 1559.
30. (a) Chang, B.-Y.; Hong, S.-Y.; Yoo, J.-S.; Park, S.-M. *J. Phys. Chem. B* **2006**, *109*, 19386. (b) Hong, S.-Y.; Park, S.-M. *J. Phys. Chem. B* **2006**, *111*, 9779.
31. (a) See, for example, Chapter 10 of Ref. 1. (b) Muzikar, M.; Fawcett, W. R. *Anal. Chem.* **2004**, *76*, 3607. (c) (a) Smith, D. E. *Electroanal. Chem.* **1966**, *1*, 1. (b) Smith, D. E. *Crit. Rev. Anal. Chem.* **1971**, *2*, 247.
32. Chang, B.-Y.; Park, S.-M. *Anal. Chem.* **2007**, *79*, 4892.
33. (a) Harrington, D. A.; van den Driessche, P. *Electrochim. Acta* **1999**, *44*, 4321. (b) Harrington, D. A. *J. Electroanal. Chem.* **1996**, *403*, 11. (c) Harrington, D. A. *J. Electroanal. Chem.* **1998**, *449*, 9.
34. http://web.uvic.ca/~dharr/impedance/manystep.htm